

Confounding oscillations: impedance mismatches distort local field potential readouts of disease

Vineet Tiruvadi^{a,b}, Sam James^a, Bryan Howell^e, Robert Gross^{a,b}, Robert Butera^a, Cameron McIntyre^{c,e}, Helen Mayberg¹

^a*Georgia Institute of Technology, Georgia, United States*

^b*Emory School of Medicine, Georgia, United States*

^c*Case Western Reserve University, Ohio, United States*

^d*Cleveland Clinic, Ohio, United States*

^e*Icahn School of Medicine at Mount Sinai, New York, United States*

Abstract

Background. Adaptive deep brain stimulation (DBS) requires chronic recordings with high recording fidelity. Changes in recording environment can distort differentially recorded local field potentials (LFPs) by affecting how well stimulation artifacts are removed. Corrections for these distortions must be made to ensure readouts accurately reflect disease state over chronic timescales.

Hypothesis/Objective. We hypothesize impedance mismatches in differential LFP recordings can introduce oscillatory distortions through amplifier *gain compression*. The objective of this study is to develop a preprocessing strategy to mitigate gain compression related distortions that can arise from impedance mismatches in chronic DBS recordings.

Methods. Impedance mismatches, chronic recording instabilities, and stimulation-locked distortions are observed in patient LFP recordings from Activa PC+S

devices. A benchtop preparation with controlled impedances was used to confirm impedance mismatch led to distortions.

Results. Patient recordings exhibit changes suggestive of gain compression. We observed dynamic impedance mismatches measured from patient leads. Using benchtop recordings, we demonstrated that resistivity differences resulted in gain compression distortions and present a preprocessing strategy to mitigate the effects of these distortions. A simplified mathematical model is provided that captures impedance mismatch related gain compression.

Conclusions. Impedance mismatches in DBS electrodes over months can lead to distortions in oscillatory measurements that can confound oscillatory readouts of disease. We present a preprocessing strategy that mitigates the effects of distortion for oscillatory analyses in contemporary devices and for future devices that record differential LFP.

Highlights.

- Oscillations from differential LFP recordings can be confounded by environmental changes
- Impedance mismatches can result in gain compression during active stimulation
- Preprocessing steps can mitigate these effects
- Mathematical modeling can identify further strategies

Keywords: Deep brain stimulation, Closed-loop, Biometric, mathematical model, impedance mismatch, readouts, differential LFPs

¹ 1. Introduction

² Deep brain stimulation (DBS) is a neurosurgical therapy for various motor [1] and psychiatric disorders [2], including treatment resistant depression

4 (TRD) [3]. Adaptive DBS is emerging as a replacement for manual DBS
5 adjustments based on clinical assessments of symptoms, so called *open-loop*
6 *therapy*. In adaptive DBS a brain readout is derived from neural recordings
7 and used to inform algorithmic changes to stimulation parameters, or *close*
8 *the loop*. This approach has already been applied to DBS indications with
9 well studied readouts like epilepsy [4] and Parkinsons Disorder [5]. Whether
10 such improvements significantly improve therapeutic efficacy in neurologi-
11 cal DBS remains unclear but their use in decoding subjective symptoms of
12 psychiatric illnesses may be crucial [6].

13 Recently developed prototype bidirectional DBS devices (bdDBS) enable si-
14 multaneous local field potential (LFP) recordings during active therapy over
15 the course of months [?]. Accurate, stable recording of disease-related
16 neural activity, or recording fidelity, is necessary for any adaptive DBS strat-
17 egy but critical characterization of recording fidelity is slowly emerging [7].
18 One crucial factor in recording fidelity is the impedance of DBS electrodes.
19 Impedances on DBS electrodes can affect the delivered stimulation [8, 9]
20 and longitudinal measurements can be important for clinical management
21 of stimulation [10]. Electrode impedances have been linked to encapsulation
22 [8], and gray/white matter composition [11, 12]. In the case of heterogeneous
23 brain targets, like the subcallosal cingulate cortex (SCC), differences in tis-
24 sue electrical properties may result in imperfect stimulation rejection. Tis-
25 sue impedance, a resistive force to current flow, can differentially weaken the
26 stimulation artifact on one electrode, which then result in imbalanced stimu-
27 lation artifact recording. This impedance mismatch can change at timescales
28 relevant to adaptive DBS and psychiatric recovery [10, 13, 14].

29 Recording LFP during stimulation is challenging due to the difference be-
30 tween small amplitude neural signals and large-amplitude stimulation. When
31 sensitive signal amplifiers receive inputs that are larger than expected, *gain*
32 *compression* can happen and the output signal is amplified less than ex-
33 pected, or *compressed*. This compression introduces predictable distortions
34 into the recording, specifically the introduction of sharp frequency peaks
35 arising from the amplifier clipping properties and broad spectrum slope flat-
36 tening []. A differential LFP enables rejection of symmetrically recorded
37 stimulation artifacts before reaching sensitive amplifier hardware. A critical
38 assumption of this strategy is that the stimulation artifact is seen equally in
39 both recording electrodes, however brain target non-uniformity may break

40 this assumption [15].

41 Here, we hypothesize that impedance mismatches can distort LFP readouts
42 through *gain compression*. First, we demonstrate that distortions present
43 in clinical LFP recordings can be ascribed to gain compression secondary
44 to impedance mismatches. We qualitatively confirmed that impedance mis-
45 matches can yield gain compression in both a mathematical model and a
46 benchtop experiment using the PC+S. We then propose and validate a pre-
47 processing pipeline to mitigate the effects of distortions. technique to con-
48 servatively remove gain compression distortions. This enables more rigorous
49 analysis and stabilization of chronic oscillatory recordings in a growing num-
50 ber of devices that rely on differential LFP recordings [15, 16].

51 **2. Methods**

52 *2.1. Regulatory, Surgery, and Clinical Assessments*

53 Six patients with severe, chronic treatment resistant depression were con-
54 sented and enrolled in an IRB and FDA approved research protocol at Emory
55 University (clinicaltrials.gov NCT01984710; FDA IDE G130107). Subjects
56 were implanted using an individualized connectome strategy targeting sub-
57 callosal cingulate white matter [17] using Medtronic 3387 DBS leads with four
58 electrodes spaced 3mm apart. Leads were connected to a prototype Activa
59 PC+S DBS system (Medtronic PLC, Minneapolis, MN) capable of differen-
60 tial LFP recordings. Patients are brought in for weekly clinical assessments
61 when recording and impedance measurements are taken.

62 *2.2. Clinical local field potentials*

63 The Activa PC+S is capable of recording local field potentials (LFPs) simul-
64 taneously with stimulation and store it for later download. Recordings are
65 sampled at 422Hz with a hardware bandpass filter of 0.5Hz and 100Hz. Two
66 channels are collected, one each from leads in bilateral SCC. Channels are dif-
67 ferentially recorded from two electrodes directly adjacent to the stimulation
68 electrode [15].

69 *2.3. Modeling differential local field potentials*

70 LFPs are generated by gray matter [18, 19]. Differential LFPs record voltages
71 from two electrodes into a differential amplifier that removes stimulation and
72 any other signals that are present in both, amplifying the remaining *difference*
73 (Figure1a).

74 A mathematical model is developed to link impedance mismatches to oscil-
75 latory distortions through the hypothesized gain compression. A simplified
76 tissue-electrode interface is fed into an idealized differential amplifier with in-
77 dependent input impedances. The resulting signal is then input into a signal
78 amplifier that models amplifier behavior, including extremes like amplifier
79 saturation.

80 *2.4. Clinical Impedance Assessments*

81 Electrode impedances are measured on all four electrodes for each implanted
82 lead at every clinical assessment. The standard clinician-controlled Medtronic
83 NVision is used to measure impedance in monopolar mode with a 100Hz
84 sine wave at 3V [20]. Resulting impedances are recorded for all electrodes
85 throughout the entire study. Differences in left and right impedances are
86 observed (Figure1b)

87 *2.5. Physical Validation*

88 Saline-agar preparations were created to assess recording fidelity under fixed
89 resistivity differences in media surrounding the DBS lead [21]. Saline phase
90 was created with 0.5 mg/mL of NaCl, while agar phase was created with
91 1mg/mL of NaCl. Agar phase was poured into a 10mL conical corning tube
92 and blue dye (Fluorophore?) was added before being placed in a 32C fridge
93 for 20 minutes. Saline phase was then added before DBS lead insertion.
94 A micromanipulator was used to insert and maintain 3387 lead location at
95 eaither uniform saline or agar-saline interface. The 3387 lead was connected
96 to a demo PC+S unit and recordings were collected using the standard clin-
97 ical sensing tablet. Impedances were measured using the NVision clinician
98 programmer.

⁹⁹ *2.6. Oscillatory analyses*

¹⁰⁰ Recordings were transformed into the frequency-domain using a Welch power
¹⁰¹ spectral density (PSD) estimate with 1024 FFT bins, 0% overlap, 844 sam-
¹⁰² ple Blackman Harris Windows. Oscillatory power is then computed as either
¹⁰³ the mean or median value of the PSD for a predefined frequency range cor-
¹⁰⁴ responding to standard oscillatory bands: δ (1-4Hz), θ (4-8Hz), α (8-14Hz),
¹⁰⁵ β (14-30Hz), γ (30-50Hz). Adjusted oscillatory band windows are proposed
¹⁰⁶ to avoid distortions. Polynomial curves are fit to logPSDs and subsequently.

¹⁰⁷ *2.7. Math modeling and library*

¹⁰⁸ An open-source library is provided that implements the proposed prepro-
¹⁰⁹ cessing strategy. A simplified mathematical model that generated simulated
¹¹⁰ LFP with gain compression distortions is provided. Two stages are imple-
¹¹¹ mented: a hardware stage that reflects the differential LFP channel and an
¹¹² analysis stage that reflect oscillatory analyses. The model is used to predict
¹¹³ the frequency-domain distortions effected by gain compression. The model
¹¹⁴ is provided as an interactive Jupyter Notebook ([link](#)).

¹¹⁵ **3. Results**

¹¹⁶ *3.1. Clinical recordings and recording environment exhibit instabilities*

¹¹⁷ First, we observed frequency changes present in clinical recordings under
¹¹⁸ fixed recording gain and variable stimulation voltages for an example pa-
¹¹⁹ tient. Large amplitudes are recorded during stimulation epochs, with larger
¹²⁰ stimulation voltages evoking larger recorded amplitudes (Figure1c, top). In
¹²¹ the time-frequency domain, stimulation voltage dependent broad increases
¹²² in power are observed in a voltage-dependent manner (Figure1c, bottom).

¹²³ Assessing recording stability under active stimulation is an important step be-
¹²⁴ fore analysing LFP and setting chronic recording gains. In the Activa PC+S
¹²⁵ specifically, a 105.5Hz clock artifact is present at fixed amplitude. Changes
¹²⁶ in clock artifact power can be used to visually assess amplifier saturation. We
¹²⁷ observe changes in clock artifact power for all patients across the 28 weeks of

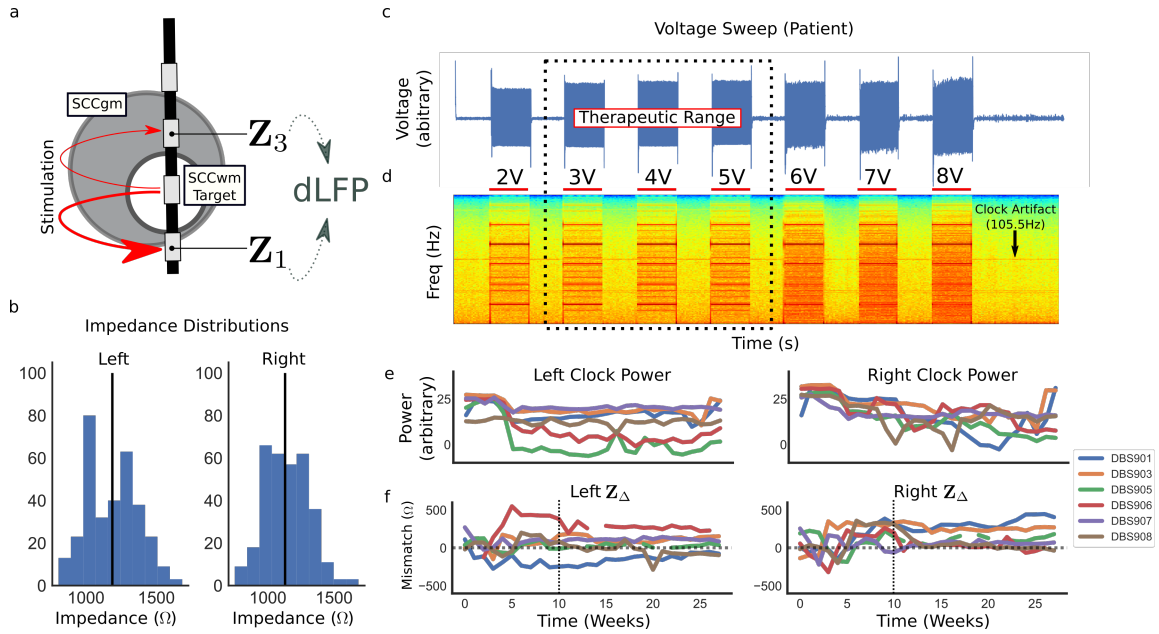


Figure 1: Differential LFP recordings and environment exhibit instabilities. a, Schematic of differential LFPs recorded around a white matter target. Two stimulation-adjacent electrodes record neural signals and stimulation artifact. b, All recorded impedances across all patients demonstrate significant variation in range as well as between sides. c, Example time-domain and time-frequency domain LFP recording from Patient 5 at different stimulation voltages. Time-domain demonstrates large changes during stimulation (top) but time-frequency domain demonstrates voltage-dependent increases in broadband activity and narrowband features. Clock artifact (105.5Hz) is a device artifact that can reflect amplifier saturation level. b, Distributions of power in clock artifact have high variance. c, Clock artifacts demonstrate instability within a patient across the study, suggesting amplifier saturation is variable. d, Impedance mismatch dynamics per week for each patient (colored lines) and the mean change across all patients (black line).

128 study, including the 24 weeks of therapy (Figure1d). (Figure??). Impedance
129 mismatches are one source that can contribute to decreases in recording fi-
130 delity and these mismatches are also observed to be dynamic over the study
131 (Figure ??).

132 Next, we observe instabilities in the recording environment reflected through
133 measured impedances. Impedances ranged from 800Ω to 1600Ω (Figure1b).
134 Impedance mismatches ranges in magnitude from 0 to 500Ω , representing
135 a significant portion of the total impedance. All patients exhibited more
136 dynamic impedances in the first ten weeks than the subsequent 10 weeks.

137 *3.2. Impedance mismatch introduces frequency-domain distortions consistent
138 with gain compression*

139 Next, we verified the link between impedance mismatch and gain compres-
140 sion using a benchtop experiment with the PC+S platform. DBS3387 leads
141 were placed in a agar-saline preparation with controlled resistivities in each
142 phase which yielded measurably different impedances (FigureA.3). A volt-
143 age sweep experiment was performed in uniform saline and at the interface
144 of saline and low resistance agar (Figure A.3a). Spectrograms visualize the
145 dLFP under both lead placements and exhibit slight variations that are dif-
146 ficult to differentiate visually (FigureA.3b). Oscillatory analyses were then
147 performed to compare PSD of recordings taken at different stimulation volt-
148 ages (Figure??). These observations were consistent with our hypothesis that
149 impedance mismatches cause distortions.

150 Finally, we sought to mathematically model the link between impedance mis-
151 match and distortions through amplifier gain compression. Using a simplified
152 model of the tissue-electrode interface, we built a model that predicted the
153 effects of distortions on the recording PSDs (Figure??). We find that the
154 model predicts the location of intermodulation harmonics when compared to
155 saline recordings and qualitatively reflects the broadband distortions.

156 *3.3. Gain compression corrections*

157 Next, we propose a preprocessing pipeline to mitigate gain compression dis-
158 tortions (Figure2a). The correction pipeline consists of taking recorded dif-

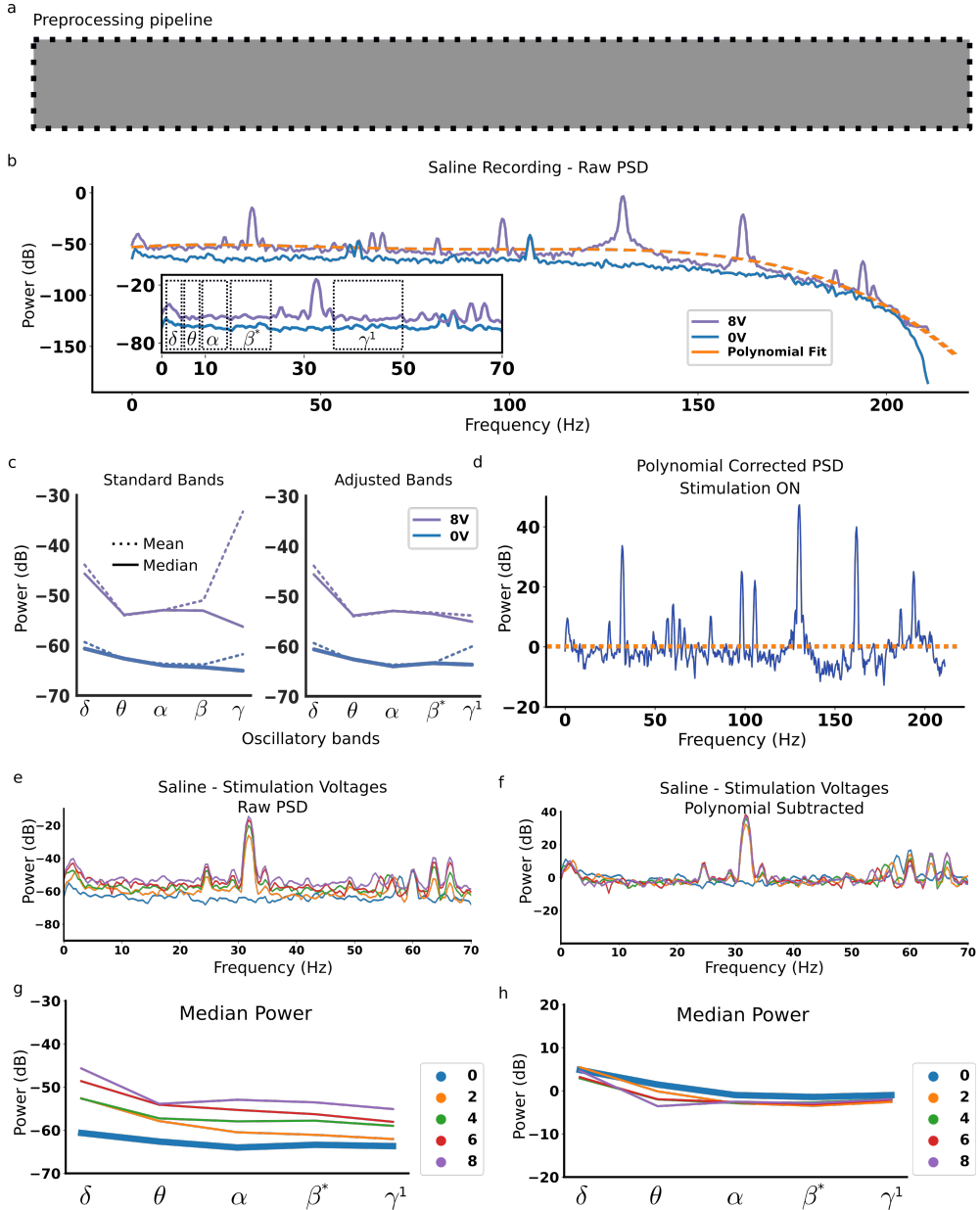


Figure 2: Corrections and adjustments for distortions. a, Saline recorded PSD during active stimulation (8V - violet), no stimulation (0 - blue), and a fourth-order polynomial fit to the PSD (orange). c, Power in the traditional oscillatory bands calculated from saline recordings using the mean (dotted) and calculated using the median power (solid). b, Power in oscillatory windows adjusted around device-specific artifacts using both area under curve (purple) and median power (blue). c, Example recording with intermodulation harmonics labeled (black) and clock artifact of PC+S (red). Polynomial fit to PSD captures broadband activity (orange dotted line). d, Polynomial corrected PSD removes broad spectrum features that can be distorted by gain compression.

159 differential LFP recordings, transforming them to PSDs and log-transforming
160 them. A polynomial curve is fit and subtracted. The resulting curve is
161 transformed out of log-space to calculate powers using either mean or me-
162 dian surrogates of power. We validated these approaches in an agar-saline
163 voltage sweep dataset (Figure2).

164 First, we suggest a median-based power calculation instead of area under
165 the curve in order to minimize the influence of narrow-band artifacts. The
166 impact of this step is most apparent when applied to the standard oscillatory
167 band powers (Figure2c, left). Oscillatory powers under 8V and 0 should be
168 identical since there are no neural sources. Median calculations more accu-
169 rately capture the γ power measured under 0 due to the median's robustness
170 to narrowband peaks.

171 Second, adjustment of oscillatory bands around the intermodulation har-
172 monics results in reduced artifacts in oscillatory power (Figure2b, inset).
173 The adjusted bands are as follows: δ (1-4Hz), θ (4-8Hz), α (8-14Hz), β^* (14-
174 25Hz), γ^1 (35-50Hz). β^* adjustments are made empirically to avoid a peak
175 in 27Hz, though this peak is not explained by gain compression distortions.
176 When mean and median powers are calculated with the adjusted bands the
177 measured oscillatory powers are closer to the 0 condition (Figure2c,right).

178 Third, polynomial subtraction from the logPSD has been used to identify
179 oscillatory activity [22] and eliminates broadband activity that is corrupted
180 by gain compression. The order of the fit polynomial was based from prior
181 literature [22] but adjusted to be a polynomial of o=4. The polynomial
182 curve is fit to a recording's logPSD (Figure2b) and subtracted (Figure2d).
183 These corrections, when applied to agar-saline recordings at various stimu-
184 lation voltages (Figure2e,g), bring the calculated oscillatory powers together
185 to match the 0V condition (Figure2f,h).

186 4. Discussion

187 Adaptive DBS requires a consistent, reliable measurement of disease state
188 through brain recordings over chronic timescales. Current strategies for
189 recording rely on differential LFP channels to enable sufficient rejection of
190 stimulation artifact. In this study we showed that impedance mismatches in

191 differential LFP channels can make recording susceptible to a form of dis-
192 tortion called *gain compression* in the presence of stimulation. Impedances
193 mismatches change over weeks and months, possibly confounding oscillatory
194 readouts of disease. We proposed a preprocessing strategy to mitigate these
195 distortions and provide the code for this strategy as an opensource toolset.

196 Impedances recorded from SCC-DBS patients demonstrated long-term impedance
197 changes consistent with previous literature [10, 13, 7]. We extend these ob-
198 servations by characterzing impedances mismatches and their dynamics at
199 timescales relevant to psychiatric symptom recovery [23]. Independently,
200 recording instabilities are measured by observing the 105.5Hz device clock
201 artifact, a constant signal that is always present in LFP recordings. Changes
202 in this constant signal can reflect changes in recording fidelity from various
203 sources, only one of which is the impedance mismatch. We did not ob-
204 serve significant correlations between these two measurements (Supplemen-
205 tary S??) but this may be because of both nonlinear relationships between
206 the two and the presence of other contributors to changes in clock power.

207 Identification of a disease-specific readout using differential LFPs must ac-
208 count for confounds in the surrounding tissue. Oscillations are susceptible
209 to gain compression distortions. In our mathematical model, we simulated
210 a constant amplitude 15Hz oscillation and observed the effects of gain com-
211 pression on changing the power in the oscillation (Supplementary Figure??).
212 One approach to account for these is presented in this paper as a prepro-
213 cessing pipeline. The steps taken in this pipeline are conservative and likely
214 remove signals from neural sources, but signals that survive this correction
215 can be reported with more confidence.

216 Our demonstration of the link between impedance mismatch and gain com-
217 pression represents a worst case scenario. There are several instances where
218 impedance mismatches may not result in significant gain compression. To
219 help facilitate this, a simulation library is provided to identify gain com-
220 pression related artifacts for a particular stimulation frequency, impedance
221 mismatch, and gain setting (github).

222 This study has several limitations. The approaches proposed here are con-
223 servative corrections that may remove brain signal along with the features
224 corrupted by gain compression. While this increases the probability of false

negatives, any signal found after these corrections can be more confidently reported. Further study is needed to extend these methods and reduce. Another limitation is in the oversimplification of the tissue-electrode interface in our mathematical model where more physiologically accurate, but more complex, models exist [12]. While justified by our focus on relating impedance mismatches to gain compression, this simplified interface limits the interpretability of the model, requiring further empirical testing for any proposed strategy. Finally, our focus was understanding one particular source of artifact and not to characterize all device-specific artifacts of the PC+S. There are several artifact peaks present in saline recordings that are unaccounted for by our model of gain compression. The mathematical model is kept general to dLFP devices and does not recapitulate the PC+S saline PSDs exactly due to the lack of knowledge of specific device parameters and the lack of detailed filter modeling deemed out of scope for studying gain compression distortions.

Despite these limitations, our results have major implications for adaptive DBS. First, LFPs are generated by gray matter but a growing class of brain targets for DBS are white matter tracts [24]. Adaptive DBS in these targets will have to optimize DBS lead placement for both delivery of therapy and recording of readout, making impedance mismatches highly likely. Second, differential LFPs are growing as a strategy for noise mitigation [16] as well as for unique signal extraction [25], making our results relevant to future scientific studies and engineering improvements. Third, the mathematical model developed to link impedance mismatch to gain compression is provided as an opensource Jupyter/Python notebook that can be used to tailor artifact predictions to study-specific parameters, hypothesized oscillations, and impedance mismatches (github.com/virati/LFP_Sim).

5. Conclusion

In this study we showed that impedance mismatches in differential LFP recording channels can result in oscillatory distortions, especially in the presence of stimulation artifacts. We then proposed and validated a methodology to mitigate these distortions. Fixing gain compression requires hardware-level advances but this work may enable limited oscillatory analyses in current-

258 generation bdDBS devices and serve as a preprocessing step for adaptive DBS
259 applications.

260 **6. References**

- 261 [1] P. S. Larson, Deep brain stimulation for movement disorders, *Neurotherapeutics* 11 (2014) 465–474. 24833244[pmid].
- 262
- 263 [2] P. E. Holtzheimer, H. S. Mayberg, Deep brain stimulation for psychiatric
264 disorders, *Annu Rev Neurosci* 34 (2011) 289–307. 21692660[pmid].
- 265
- 266 [3] M. P. Dandekar, A. J. Fenoy, A. F. Carvalho, J. C. Soares, J. Quevedo,
267 Deep brain stimulation for treatment-resistant depression: an integrative
268 review of preclinical and clinical findings and translational implications,
269 *Molecular Psychiatry* 23 (2018) 1094 EP –. *Mechanisms of Drug Action*.
- 270
- 271 [4] F. T. Sun, M. J. Morrell, R. E. Wharen, Responsive cortical stimulation
for the treatment of epilepsy, *Neurotherapeutics* 5 (2008) 68–74.
- 272
- 273 [5] N. C. Swann, C. de Hemptinne, M. C. Thompson, S. Miocinovic, A. M.
274 Miller, R. Gilron, J. L. Ostrem, H. J. Chizeck, P. A. Starr, Adaptive
275 deep brain stimulation for parkinsons disease using motor cortex sensing,
Journal of Neural Engineering 15 (2018) 046006.
- 276
- 277 [6] O. G. Sani, Y. Yang, M. B. Lee, H. E. Dawes, E. F. Chang, M. M.
278 Shanechi, Mood variations decoded from multi-site intracranial human
brain activity, *Nature Biotechnology* 36 (2018) 954 EP –.
- 279
- 280 [7] N. C. Swann, C. de Hemptinne, S. Miocinovic, S. Qasim, J. L. Ostrem,
281 N. B. Galifianakis, M. San Luciano, S. S. Wang, N. Ziman, R. Taylor,
282 et al., Chronic multisite brain recordings from a totally implantable
283 bidirectional neural interface: experience in 5 patients with parkinson’s
disease, *Journal of neurosurgery* 128 (2018) 605–616.
- 284
- 285 [8] C. R. Butson, C. B. Maks, C. C. McIntyre, Sources and effects of
286 electrode impedance during deep brain stimulation, *Clin Neurophysiol*
117 (2006) 447–454. 16376143[pmid].

- 287 [9] S. Miocinovic, S. F. Lempka, G. S. Russo, C. B. Maks, C. R. Butson,
288 K. E. Sakaie, J. L. Vitek, C. C. McIntyre, Experimental and theoretical
289 characterization of the voltage distribution generated by deep brain
290 stimulation, *Experimental Neurology* 216 (2009) 166 – 176.
- 291 [10] J. Wong, A. Gunduz, J. Shute, R. Eisinger, S. Cernera, K. W. D. Ho,
292 D. Martinez-Ramirez, L. Almeida, C. A. Wilson, M. S. Okun, C. W.
293 Hess, Longitudinal follow-up of impedance drift in deep brain stimula-
294 tion cases, *Tremor Other Hyperkinet Mov (N Y)* 8 (2018) 542–542.
295 29607241[pmid].
- 296 [11] D. Satzer, E. W. Maurer, D. Lanctin, W. Guan, A. Abosch, Anatomic
297 correlates of deep brain stimulation electrode impedance, *Journal of
298 Neurology, Neurosurgery & Psychiatry* 86 (2015) 398–403.
- 299 [12] S. F. Lempka, S. Miocinovic, M. D. Johnson, J. L. Vitek, C. C. McIntyre,
300 In vivo impedance spectroscopy of deep brain stimulation electrodes,
301 *Journal of Neural Engineering* 6 (2009) 046001.
- 302 [13] D. Satzer, D. Lanctin, L. E. Eberly, A. Abosch, Variation in deep brain
303 stimulation electrode impedance over years following electrode implan-
304 tation, *Stereotact Funct Neurosurg* 92 (2014) 94–102. 24503709[pmid].
- 305 [14] K. A. Sillay, J. C. Chen, E. B. Montgomery, Long-term measurement of
306 therapeutic electrode impedance in deep brain stimulation, *Neuromod-
307 ulation: Technology at the Neural Interface* 13 (2010) 195–200.
- 308 [15] S. Stanslaski, P. Afshar, P. Cong, J. Giftakis, P. Stypulkowski, D. Carl-
309 son, D. Linde, D. Ullestad, A. Avestruz, T. Denison, Design and valida-
310 tion of a fully implantable, chronic, closed-loop neuromodulation device
311 with concurrent sensing and stimulation, *IEEE Transactions on Neural
312 Systems and Rehabilitation Engineering* 20 (2012) 410–421.
- 313 [16] S. Stanslaski, J. Herron, T. Chouinard, D. Bourget, B. Isaacson, V. Kre-
314 men, E. Opri, W. Drew, B. Brinkmann, A. Gunduz, T. Adamski,
315 G. Worrell, T. Denison, A chronically-implanted neural coprocessor
316 for exploring treatments for neurological disorders, *IEEE Transactions
317 on Biomedical Circuits and Systems* (2018) 1–1.
- 318 [17] P. Riva-Posse, K. S. Choi, P. E. Holtzheimer, A. L. Crowell, S. J. Gar-
319 low, J. K. Rajendra, C. C. McIntyre, R. E. Gross, H. S. Mayberg, A

- 320 connectomic approach for subcallosal cingulate deep brain stimulation
321 surgery: prospective targeting in treatment-resistant depression, Molecular
322 Psychiatry 23 (2017) 843 EP –. Original Article.
- 323 [18] B. Pesaran, Uncovering the mysterious origins of local field potentials,
324 Neuron 61 (2009) 1 – 2.
- 325 [19] O. Herreras, Local field potentials: Myths and misunderstandings, Front
326 Neural Circuits 10 (2016) 101–101. 28018180[pmid].
- 327 [20] A. R. Kent, B. D. Swan, D. T. Brocker, D. A. Turner, R. E. Gross,
328 W. M. Grill, Measurement of evoked potentials during thalamic deep
329 brain stimulation, Brain Stimul 8 (2015) 42–56. 25457213[pmid].
- 330 [21] M. A. Kandadai, J. L. Raymond, G. J. Shaw, Comparison of electrical
331 conductivities of various brain phantom gels: Developing a brain gel
332 model, Materials Science and Engineering: C 32 (2012) 2664 – 2667.
- 333 [22] D. D. Wang, C. de Hemptinne, S. Miocinovic, S. E. Qasim, A. M. Miller,
334 J. L. Ostrem, N. B. Galifianakis, M. S. Luciano, P. A. Starr, Subthalamic
335 local field potentials in parkinson’s disease and isolated dystonia: An
336 evaluation of potential biomarkers, Neurobiology of Disease 89 (2016)
337 213 – 222.
- 338 [23] A. L. Crowell, S. J. Garlow, P. Riva-Posse, H. S. Mayberg, Characterizing
339 the therapeutic response to deep brain stimulation for treatment-
340 resistant depression: a single center long-term perspective, Frontiers in
341 Integrative Neuroscience 9 (2015) 41.
- 342 [24] J. M. Henderson, ”connectomic surgery”: diffusion tensor imaging (dti)
343 tractography as a targeting modality for surgical modulation of neural
344 networks, Front Integr Neurosci 6 (2012) 15–15. 22536176[pmid].
- 345 [25] J.-C. Comte, G. Meyer, J. Carpocny, P. A. Salin, Differential recordings
346 of local field potential: A genuine tool to quantify functional connectivity,
347 bioRxiv (2018).

348 **Appendix A. Supplementary**

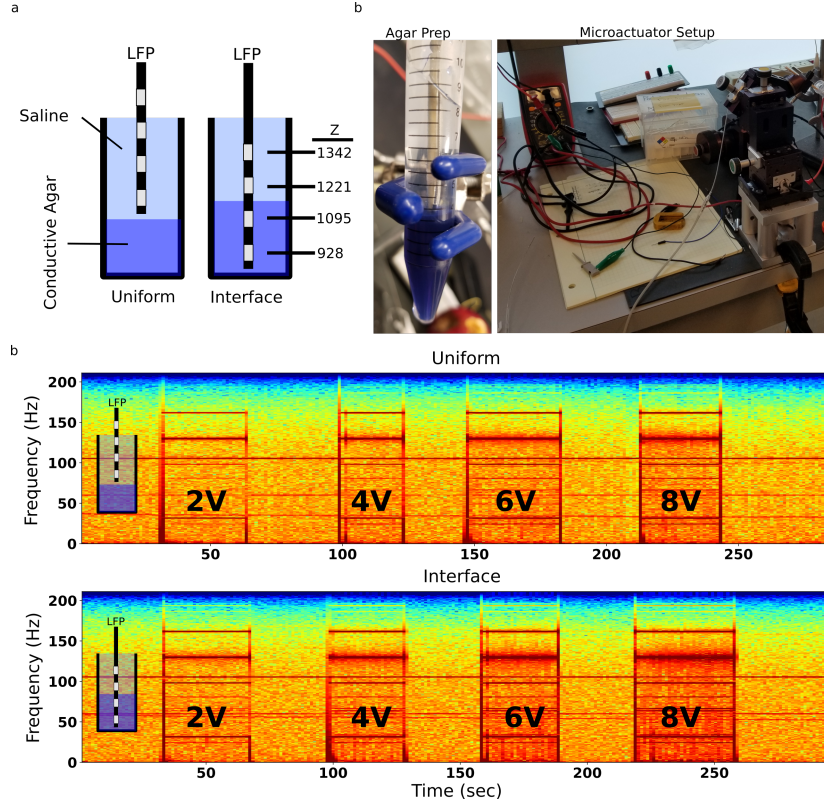


Figure A.3: Benchtop voltage sweep at different impedance mismatches a, A preparation with both saline and agar phases is constructed to establish a fixed impedance mismatch. b, Left: Example preparation with dye demarcating the low resistivity agar phase. Right: Benchtop experimental setup with micromanipulator enabled precise placement of DBS lead into interface of agar and saline phases. c, Time-frequency plots for experimental voltage sweep run in uniform saline phase and at the interface of saline and agar. Stimulation voltages are at: 0, 2V, 4V, 6V, 8V.

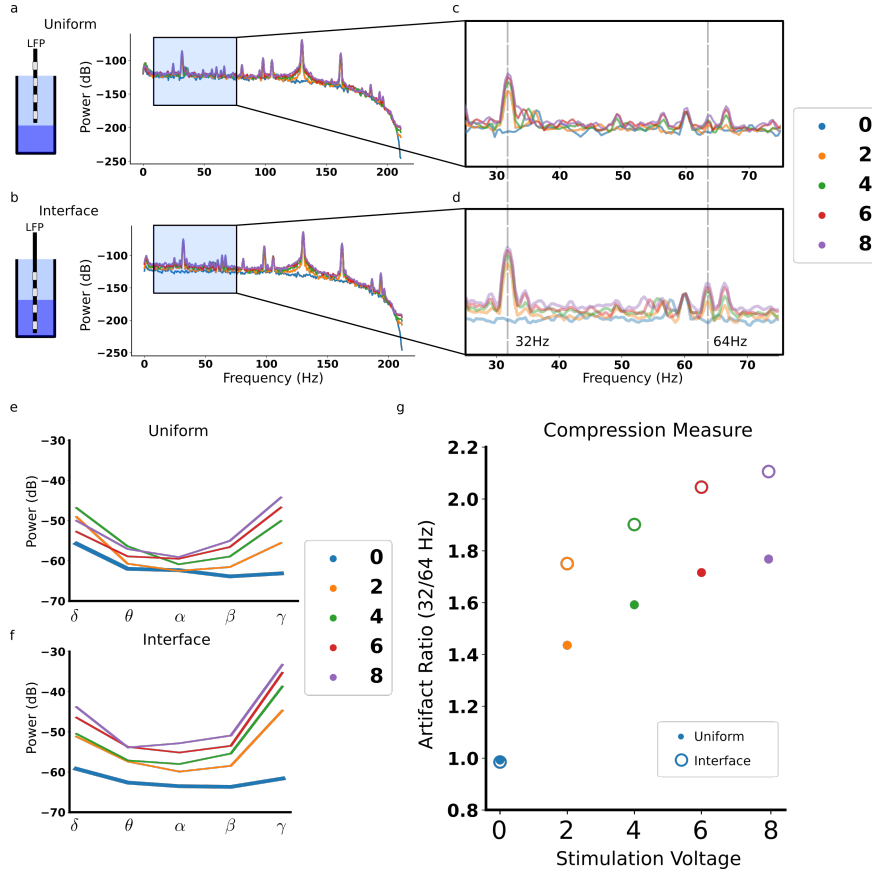


Figure A.4: Benchtop impedance mismatches evoke predicted gain compression distortions

a, PSD in the uniform medium and b, interface. Colors correspond to stimulation at different voltages. c,d Focus on 30-70Hz range demonstrates the effect that stimulation voltage has on recorded PSD. e, Oscillatory band power changes at different stimulation voltages are exaggerated when f, recording from the interface. g, Ratio of 32/64Hz power at different stimulation voltages

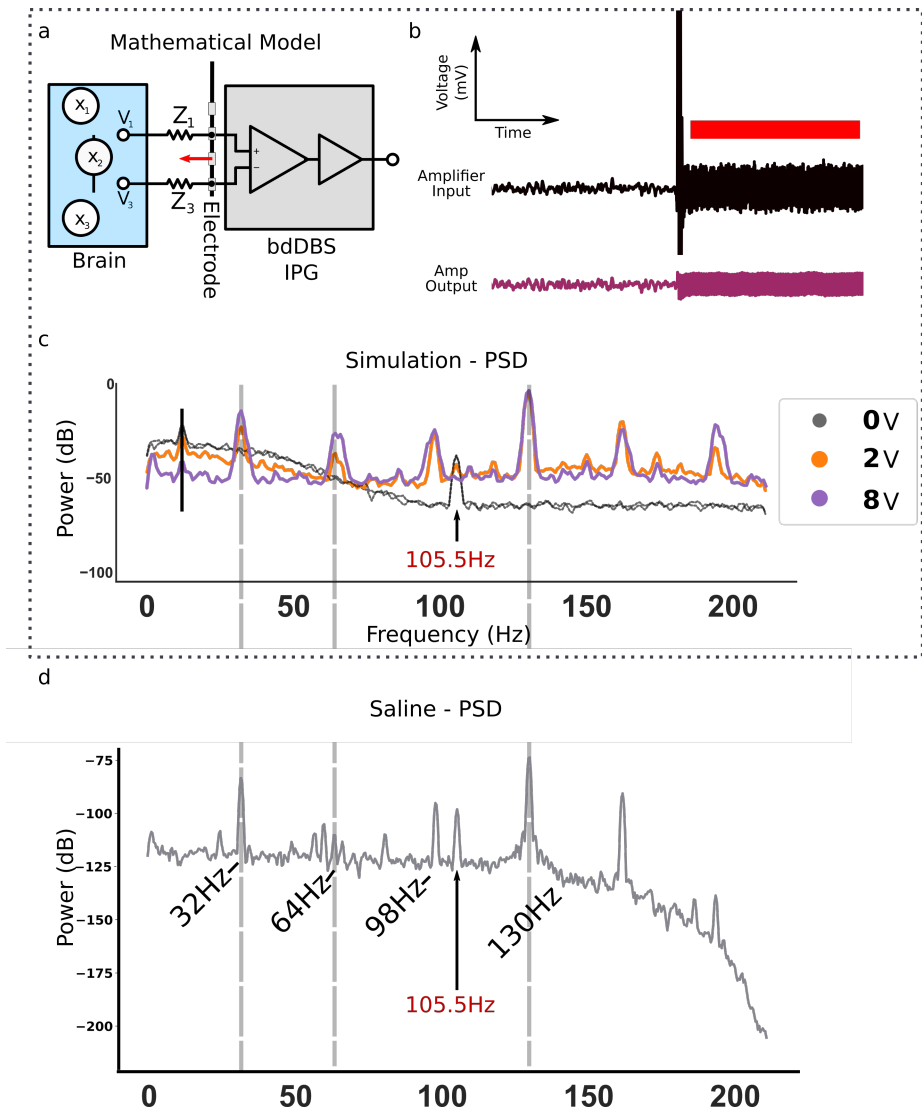


Figure A.5: Mathematical model identifies location of distortions in dLFP

a, Model of differential LFP recording with simplified tissue-electrode interface. Stimulation is delivered (red arrow) and recordings are taken from adjacent electrodes with impedances Z_1 and Z_3 . b, For fixed impedance mismatch of 200Ω simulated stimulation evokes stereotypical gain compression distortions: emergence of intermodulation harmonics (32Hz and 64Hz labeled) and broad flattening of slope.